OVERVIEW OF THE FTU RESULTS

F. ALLADIO, B. ANGELINI, M.L. APICELLA, G. APRUZZESE, E. BARBATO, M.R. BELFORTE[1], L. BERTALOT, A. BERTOCCHI, M. BORRA, G. BRACCO, A. BRUSCHI[2], G. BUCETI, P. BURATTI, A. CARDINALI, C. CASTALDO[1], C. CENTIOLI, R. CESARIO, P. CHUILON, C. CIANFARANI[1], S. CIATTAGLIA, S. CIRANT[2], V. COCILOVO, F. CRISANTI, R. DE ANGELIS, F. DE MARCO, B. ESPOSITO, M. FINKENTHAL[3] , K.B. FOURNIER[4] D. FRIGIONE, L. GABELLIERI, G. GATTI, E. GIOVANNOZZI, W.H. GOLDSTEIN[4], C. GOURLAN, F. GRAVANTI, G. GRANUCCI[2], B.C. GREGORY[5], M. GROLLI, F. IANNONE, H. KROEGLER, M. LEIGHEB, G. MADDALUNO, G. MAFFIA, M. MARINUCCI, M. MAY[3], G. MAZZITELLI, P. MICOZZI, F. MIRIZZI, F.P. ORSITTO, D. PACELLA, L. PANACCIONE, M. PANELLA, V. PERICOLI-RIDOLFINI, L. PIERONI, S. PODDA, G.B. RIGHETTI, **F. ROMANELLI**, F. SANTINI, M. SASSI, S.E. SEGRE[6], A.SIMONETTO[2], E. STERNINI, C. SOZZI[2], N. TARTONI, B. TILIA, A. A. TUCCILLO, O. TUDISCO, V. VITALE, G. VLAD, V. ZANZA, M. ZERBINI, F. ZONCA

Associazione EURATOM-ENEA sulla Fusione
C.R. Frascati
00044, Frascati, Roma, Italy

Abstract.

An overview of the Frascati Tokamak Upgrade results during the period 1996-1998 is presented. Most of the activity has been devoted to the investigation of the electron heat transport with flat/nonmonotonic safety factor profiles. Up to 14 keV of electron temperature have been obtained using electron cyclotron resonance heating (ECRH) on the current ramp. The transport analysis shows a very low electron heat transport in the region with flat/nonmonotonic safety factor profile. The electron thermal conductivity is strongly dependent on the MHD activity and it drops to values of the order $0.1 m^2/s$ in the absence of MHD fluctuations. Upon varying the resonance position in steady state conditions the effect of the ECRH on the sawtooth stabilization has been also investigated. Lower hybrid current drive studies have been performed in order to investigate the dependence of the current drive efficiency with density. Previous results of the Alcator C tokamak pointed out that at high density rather low efficiency values were obtained. The investigation carried out on FTU shows that such a result can be explained as due to the electron temperature dependence of the current drive efficiency. No degradation of the current drive efficiency is indeed observed on FTU even at density values of the order $10^{20} m^{-3}$. Ion Bernstein wave (IBW) heating studies have been also carried out in order to check the behaviour of wave-plasma coupling which is found in agreement with linear theory. Finally, impurity transport studies have been carried out. It has been possible to have a direct measurement of the flux of Mo33 which turns out to be in agreement with the expectation of quasilinear theory.

1. INTRODUCTION

After a major shutdown during 1995 for the insertion of the toroidal limiter, the Frascati Tokamak Upgrade (FTU) (B=8T, I≤1.6MA, a=0.3m, R=1.3m) restarted the operations in the first half of 1996. The heating systems became operational during 1996-1997. At present, the Lower Hybrid system (8GHz, t_{pulse}=1s) is made by 5 gyrotrons (1MW each at the generator)

---

[1] ENEA fellowship
[2] Associazione EURATOM-ENEA-CNR sulla FusioneMilano, Italy
[3] The John Hopkins University, Baltimore, MD 21218
[4] Lawrence Livermore Ntaional Labortories, Livermore, CA 94550
[5] Institut National de la Recerche Scientifique (INRS), Montreal, Canada
[6] INFM and II Università di Roma "Tor Vergata"

feeding 5 grills on two FTU windows. The maximum power delivered so far to the plasma is 1.7MW. The new electron cyclotron resonance heating (ECRH) system has been completed during the first half of 1998. It consists of 4 gyrotrons (140GHz, 0.5MW, t_{pulse}=0.5s) with a launching system which allows to inject power at oblique angle to perform Current Drive (ECCD). So far, the maximum injected power has been 0.8MW. The Ion Bernstein Wave (IBW) Heating system (433MHz, t_{pulse}=1s) is at present fed by one klystron. The maximum power coupled so far has been 0.35MW.

With the heating systems described above, FTU is characterized by dominant electron heating, contrary to most of the present tokamaks which have dominant ion heating. Furthermore, the localized ECRH absorption makes possible a detailed investigation of electron transport. Most of the activity carried out so far has been devoted to the investigation of the electron transport in the presence of flat/nonmonotonic safety factor profiles obtained by a fast ramp of the plasma current. Upon heating the plasma by ECRH in order to slow down the current density evolution, it has been possible to achieve up to 14keV electron temperature with 0.7 MW of ECRH power deposited in the plasma center at a line average density $n_e=0.36\cdot10^{20}m^{-3}$. The value of the electron thermal diffusivity in the region characterized by low/negative magnetic shear is comparable with that obtained in ohmic discharges at similar values of density and current. It is remarkable that such a low value of the diffusivity is obtained in conditions characterized by a large value of the electron temperature and temperature gradient. The electron transport is further reduced when the MHD activity is quenched. This occurs when the minimum of the safety factor is close to an integer value. In these conditions, an electron heat diffusivity as low as $\chi_e=0.1m^2/s$ is measured in the presence of a central temperature of 8keV. These results point out the crucial role played by the electromagnetic fluctuations in affecting the electron transport in the presence of flat/inverted safety factor profiles.

The ECRH is also particularly useful to test the effect of a localized perturbation in the resistivity on the global MHD stability. Transient sawtooth stabilization has been obtained by heating near the inversion radius.

An important part of the FTU activity has been devoted to the lower hybrid current drive (LHCD) studies in order to check the expected behaviour of the LHCD efficiency at high density. Previous results from high magnetic field tokamaks showed rather low values of the efficiency at reactor relevant densities. On FTU, LHCD studies have been performed in a wide range of density and magnetic field values. In the case, relevant for these studies, of wave accessibility to the plasma center, the FTU results show no degradation of the efficiency at high density and seems to point out a dependence of the efficiency on the electron temperature in qualitative agreement with the expectations of quasilinear theory. This result is further supported by a comparison with the results of several tokamaks.

In the paper the coupling results of the IBW experiment will be also outlined. The IBW experiment in FTU has the unique feature of using a waveguide array as a launching system. This minimizes the interaction with the plasma. Indeed, no significant impurity influx has been observed during IBW injection. The results are consistent with the predictions of linear theory of wave-plasma coupling.

The last subject outlined in the paper is the investigation of impurity transport. This is part of a collaborative effort with Lawrence Livermore National Laboratory and the John Hopkins University. The idea underlying this study is that at sufficiently small impurity concentration, impurities are simply advected in the background turbulence and the analysis of their transport behaviour can provide information on the turbulent fluctuations causing transport. It can be shown indeed that the impurity flux can be written exactly as the sum of a diffusive and a convective part, with the diffusion coefficient D and the convective velocity V being independent of the impurity density. The impurity flux has been obtained in a direct way by measuring the intensity of spectral lines emitted by $Mo^{32+,}$ Mo^{31+} and $Mo^{30+,}$ and assuming steady state conditions. Remarkably, the obtained radial profiles of D and V also explain the behaviour of Mo ions at lower charge state. This result is consistent with the expectations of a simple calculation based on quasilinear theory.

2. TRANSPORT AND MHD STUDIES WITH ECRH ON FAST CURRENT RAMPS

Up to 800 kW of ECRH power at 140 GHz [1] have been injected during the current ramp-up phase of 700 kA plasma discharges. Heating at the fundamental frequency, with

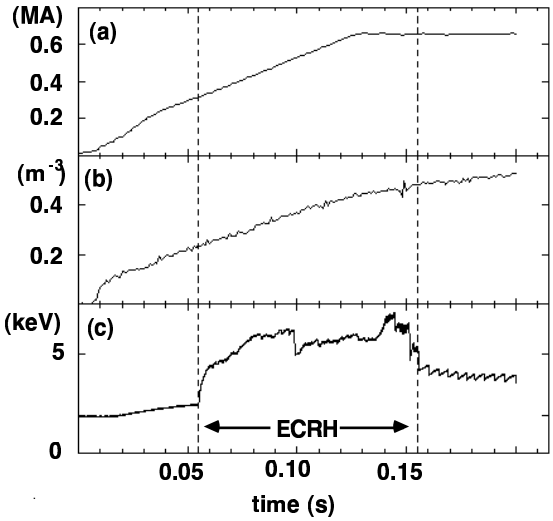

*FIG. 1 Fast current ramp time traces, pulse 12799, 360 kW ECRH: (**a**) plasma current (**b**) central line averaged density (**c**) electron temperature at R=0.97 m, from ECE polycromator.*

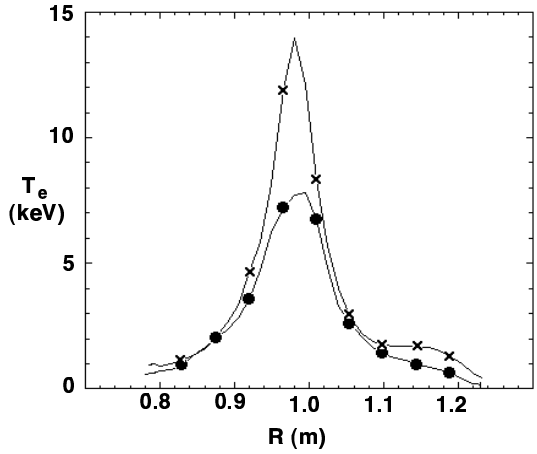

FIG. 2 Electron temperature profiles at t = 0.095 s; full points: pulse 12658, 350 kW ECRH power, hollow initial current profile; crosses: pulse 14669, 690 kW ECRH power, peaked initial current profile.

perpendicular, low field side launch with ordinary polarisation has been used, so that the resonant magnetic field B_T is 5 T. By changing B_T both on-axis and off-axis experiments have been performed. The fast current ramp-up scenario (5 MA/s, Fig. 1) has been selected because it is characterised by a variety of the current density profiles (depending on the pre-ECRH current profile and on the impurity content), going from very peaked cases when sawtooth or m=1 MHD activity can be detected already at t=0.050 s, before ECRH injection, to very broad or hollow cases, that often terminate with a reconnection consistent with double-tearing modes at resonance surfaces characterised by an integer q value. In this scenario the ECRH experiments have produced very high peak electron temperature, up to 14 keV for 690 kW injected power, Fig. 2. Due to localisation and the full absorption of the injected power, these experiments allow to perform a quantitative analysis of the energy transport in a plasma condition where the energy transport is dominated by the electron channel (due to the low density, the electron-ion coupling is very weak) and the magnetic shear values change significantly. The information on the current density profile is obtained by the solution of the diffusion equation for the poloidal magnetic field using Spitzer resistivity evaluated from the electron temperature measured by ECE diagnostics. It has been checked that the results are consistent with the MHD behaviour of the discharges, that has been studied extensively.

2.1 Transport analysis

When ECRH is localised at the plasma centre high electron temperatures are obtained, Fig.2, both for hollow and peaked pre-ECRH current density profiles. The time history of the two cases are different. The hollow pre-ECRH current profiles remain hollow during the initial phase of the additional heating and induce a crash due to the double tearing activity, when the q=2 surface enters the plasma, at t=0.1 s in Fig. 1(c).
In the cases of peaked pre-ECRH current profiles, the electron temperature reaches a maximum, followed by a degradation and eventually by the onset of the sawtooth activity. This last situation was characterised by m=1 MHD activity even in the pre-ECRH phase.

In on-axis heating experiment the interpretative local transport analysis shows (Fig. 3) that the value of the effective electron thermal diffusivity in the plasma core is in the range $0.2 \div 0.3$ m^2/s, rather independently of the detail of the q profile, even if in the case of broader current profile also the region of lower electron thermal diffusivity appears to be broader. The interpretative analysis results are meaningful only in the plasma core, excluding the narrow ECRH deposition region ($\approx$ 2 cm FWHM). In the more external plasma region the local analysis is made difficult by the role of the radiation and the uncertainty on the ohmic power evaluation

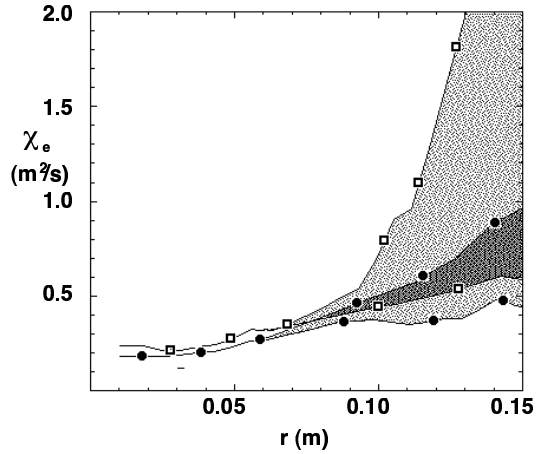

FIG. 3 Radial profile of the electron thermal diffusivity in the plasma core at t= 0.095 s; full points: pulse 12658, 350 kW ECRH power; squares: pulse 14669, 690 kW ECRH power. Shaded area indicate the uncertainity on the diffusivity value.

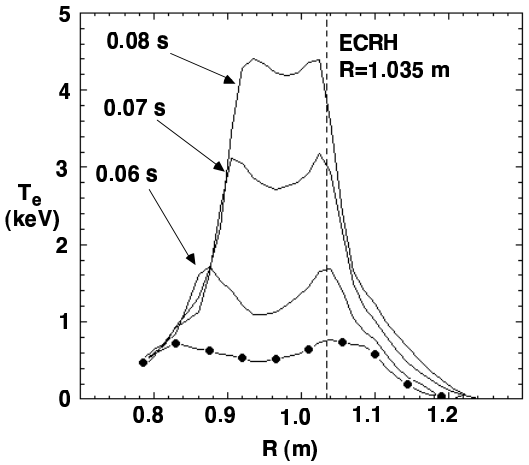

FIG. 4 Electron temperature profiles at times marked on the plot for the pulse 12953, 325 kW off-axis ECRH power; the full points indicates the pre-ECRH profile.

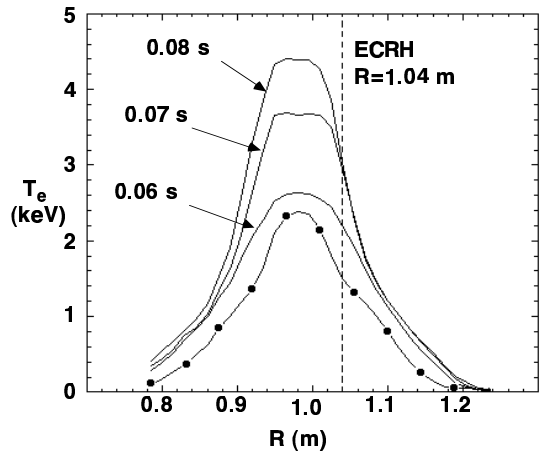

FIG. 5 Electron temperature profiles at times marked on the plot for the pulse 12616, 290 kW off-axis ECRH power; the full points indicates the pre-ECRH profile.

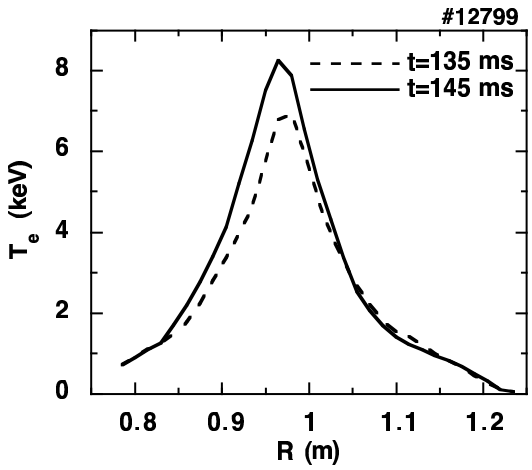

FIG. 6 Profile variation during the temperature rise at $q_{min} \approx 1$.

in the transient conditions characterising the fast current ramps, as indicated by the shaded area in Fig. 3. This last difficulty prevents also a precise evaluation of the global energy confinement of these discharges, that are also characterised by high Z_{eff} value, due to the high current and low density situation.

In ECRH off-axis experiments the plasma attains lower temperature values compared to the on-axis cases, as the additional heating is distributed on a larger volume. In off-axis experiments plasma discharges having pre-ECRH peaked or hollow current profiles behave qualitatively in different ways. In the case of a hollow initial current profile, Fig.4, the temperature profile remains hollow during the ECRH, showing a trend to become flat in the region inside the ECRH deposition layer. This behaviour can be considered as the mark of an underlying diffusive transport mechanism that can be described by a local thermal diffusivity. In the case of plasma discharges having peaked pre-ECRH profiles, the electron temperature profile remains peaked, Fig. 5. The behaviour could be qualified as non-diffusive or the sign of the existence of a inward energy pinch mechanism. Nevertheless it can also be explained by the effect of the residual ohmic heating, that in this case is peaked while it was itself hollow in the

case of a hollow pre-ECRH current profile. Indeed the different qualitative behaviour has been reproduced by simulating, [2], the two kind of discharges using the Bohm term from the electron thermal diffusivity of one of the recently proposed Bohm/Gyro-Bohm models [3]. In that framework, the residual ohmic heating plays the key role in controlling the shape of the plasma temperature for the off-axis heating scenario. Both experiments have been performed at low ECRH power, ≈300 kW, so that future experiments at a higher power level will provide a better insight on this question.

2.2 MHD analysis

The MHD behaviour of FTU discharges with peaked pressure profile and negative or low magnetic shear in the plasma core is a relevant issue as it affects the core confinement properties. This is not surprising, since the low magnetic shear ($s=rq'/q$) reduces the line bending stabilizing effect, and the local poloidal beta ($\beta_p(r)=2\mu_0(<p>-p(r))/B_p(r)^2$, $<>$ being the volume average within the radius r) reaches values $\beta_p>3$. Current ramps with central ECRH are particularly interesting as the minimum q value (q_{min}) slowly decreases from $q_{min}>3$ to $q_{min}=1$.

The main features of MHD activity can be found in Fig. 1. The sharp drop occurring at t=99 ms is caused by an m/n=2/1 double tearing instability that grows at $q_{min}\approx2$, [4], while the rapid oscillations starting at t=150 ms are m/n=1/1 sawtooth precursors. Besides these well identified features, erratic T_e fluctuations with 2÷5% amplitude are present during most of the ECRH pulse. At t≈135 ms (a short time before the appearance of m=1 precursors, i.e. when $q_{min}\approx1$), the temperature evolution reverts from fluctuating to monotonically increasing. In the next subsections, the main observations on the double tearing instability will be summarized, and the possible origin of macroscopic temperature fluctuations will be discussed.

*2.2.1. Double tearing mode*s

The evolution of double tearing modes during current ramps with ECRH features a clear branching: a precursor oscillation, lasting for 0.5 ms, is followed by a sudden growth acceleration, leading either to full reconnection in less than 25 ms, or to a large saturated oscillation that reduces the central temperature but leaves a peaked profile. The structure of precursor and saturated oscillations is a displacement with even parity, which affects more than one third on the plasma radius [5]. The fast time scale and the global nature of the perturbation imply that the mode must be ideally unstable, or at least marginally unstable [4]. The full reconnection case is similar to a sawtooth crash (apart from the wider radial extent), while the saturated oscillation resembles the so called subordinate sawtooth relaxation, with the remarkable exception that the mode structure is m/n=2/1 (the mode numbers can be unambiguously identified as the large oscillation is detected by the Mirnov coils).

The behaviour of double tearing modes is well correlated with the temperature profile shape before ECRH (the profiles before the double tearing are very similar in all cases): strongly hollow initial profiles are associated with full reconnection, while moderately peaked profiles result in small saturated oscillations. According to resistive diffusion calculations, discharges with full reconnection are characterized by a wider negative shear region; however, the precursor oscillation is quite similar in both cases. If the initial profile is peaked enough, $q_{min}<2$ already before ECRH, and the double tearing mode is not observed.

2.2.2. Macroscopic temperature fluctuations

The erratic T_e fluctuations observed during central ECRH play a role in heat transport, in fact, as the temperature evolution reverts from fluctuating to monotonically increasing at $q_{min}\approx1$, the thermal energy in the plasma core increases at a rate amounting to 60÷70% of the local heating power. This indicates that an effective transport barrier sets in when the fluctuations are suppressed. Profile evolution shows that the barrier extends throughout the plasma core [Fig. 6]. Time dependent transport analysis gives a factor two reduction of the heat diffusivity during the temperature rise. A similar suppression of electron heat transport at $q_{min}\approx1$ is observed in MHD quiescent post-pellet plasma; in this case, the low electron heat trasport regime survives for at least one confinement time [6].

The existence of a pause at $q_{min}\approx1$ points to a causal role played by MHD modes excited at $q_{min}=m/n$ resonances with relatively low m, n, in fact the distribution of such resonances features larger gaps around integer q values. As the poloidal magnetic field increases in the central region on the resistive diffusion time scale, q_{min} slowly decreases and sequentially crosses low order rational values and gaps; when q_{min} is close to a low order resonance, a temperature drop occurs, while, if q_{min} is in a gap, the peak temperature rises since the modes are effective only if they resonate in the zero shear region. This view is enforced by the observation that a strong temperature rise is also observed at $q_{min}\approx2$ when the 2/1 double tearing mode is weak [6]. Furthermore, in some cases, MHD oscillations are directly observed in conjunction with temperature drops [5]. The concept of effective transport barriers associated with the gaps around integer q values does not apply to monotonic q profiles, as in that case gaps and resonances are closely packed together.

3. LOWER-HYBRID CURRENT DRIVE

The FTU experimental programme with Lower Hybrid (LH) radiofrequency power system has been devoted to provide detailed information on the issue of the generation of toroidal current in the high plasma density regimes foreseen for ITER (line averaged density $\bar{n}_e\approx1\times10^{20}$ m^{-3}). The FTU experiment is particularly suited for this purpose, because its high toroidal field and its high LH frequency, f_0=8 GHz [7], allow to minimise the negative effects on the current drive (CD) efficiency previously found at high density. The CD efficiency is defined as $\eta_{CD}=I_{LH-}n_eR/P_{LH}$ [$10^{20}m^3A/W$], where I_{LH} (MA) is the LH driven current, R (m) is the tokamak major radius and P_{LH} (MW) is the coupled LH power.

Most of the experimental activity has been devoted to study the behaviour of the LH current drive (LHCD) efficiency at high plasma density. Previous results obtained on Alcator C [8] at high density showed a rather low efficiency η_{CD}=0.12 for B_T=10 T, as compared with that achieved, at much lower densities, on the largest tokamaks such as JET [9] or JT-60 [10], where η_{CD}=0.3 at $\bar{n}_e = 0.2\times10^{20}m^{-3}$. On the other hand, quasi linear theory predicts no degradation of the efficiency with increasing density: the suprathermal electron tail should be quenched almost linearly with n_e.

The results obtained on FTU, where η_{CD}=0.21 for effective ion charge Z_{eff}=1, show that the possibility exists to attain efficiencies as high as those on JET or JT-60 also at high density. The reason for the discrepancy with the Alcator C results can be attributed to the favourable scaling of η_{CD} with $\langle T_e\rangle$, the volume averaged electron plasma temperature. Indeed, the main difference between FTU and Alcator C is that substantially higher T_e values are achieved in FTU, with peak values $T_{e0}>$ 2.0 keV on FTU against $T_{e0}\approx0.6$ keV on Alcator C. [8, 11]. The enhancement of η_{CD} with T_e can be inferred not only from data taken on a single device [9,10], but it is also evident from the comparison between various tokamaks operating in quite different regimes, as illustrated below.

The LHCD efficiency studies have been performed on FTU in the following ranges: $0.3\le\bar{n}_e\le1.15\times10^{20}$ m^{-3}, $0.2\le P_{LH}\le1.1$ MW, $0.22\le I_p\le0.5$ MA, $4\le B_T\le7.1$ T. No operational limit was met so far due to impurity influx: LH pulses with a transmitted power density at the grill mouth larger than 10 kW/cm^2 and longer than 0.7 s are routinely and safely run, even at the highest P_{LH} achieved so far, i.e. P_{LH}=1.7 MW [12].

The LH power routinely available so far has allowed to achieve a full CD phase only for $\bar{n}_e=0.5\times10^{20}$ m^{-3}; for higher density only partial CD is obtained. A relevant example of the time evolution of the main plasma quantities is given in Fig. 7. The LH power sustains steadily the plasma current for more than 0.5 s (the estimated inductive time scale $\tau_{L/R}$ is 0.4 s) at $\bar{n}_e$ $=0.45\times10^{20}$ m^{-3}, central value $n_{e0}=0.7\times0^{20}$ m^{-3}, and $T_{e0}\approx4$ keV upon stabilisation of the

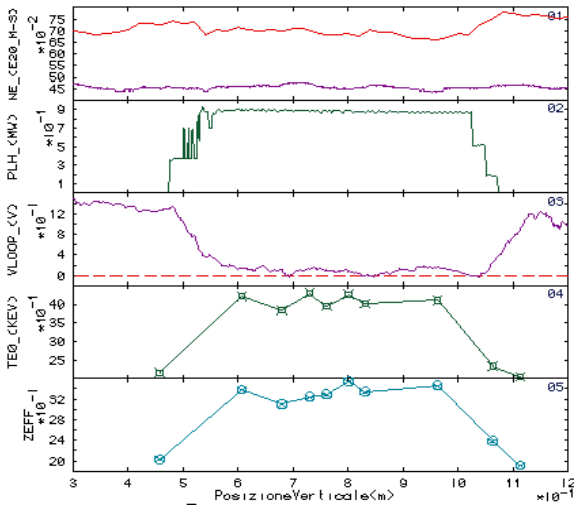

FIG.7 Temporal evolution of the main plasma quantities during a full CD phase at relatively low density. a) Line averaged and peak plasma density; b) Coupled lower hybrid power; c) Loop voltage which is maintained at zero for about 0.5 s; d) Central electron temperature; e) Average ion charge, Z_{eff}

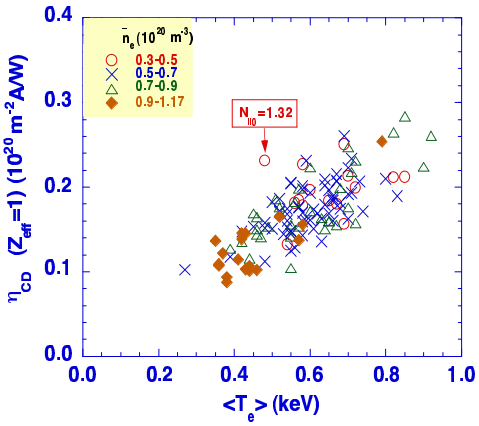

FIG. 8 Behaviour of the CD efficiency versus <T_e> for the whole data set of FTU, with $\bar{n}_e \approx 1.17\times10^{20}$ m^{-3}. $N_{||0}$=1.52 and 1.82 unless otherwise specified

sawtooth activity. For higher density a drop up to 50% of the loop voltage V_l with T_{e0}> 2 keV has been achieved at $\bar{n}_e=0.9\times10^{20}$ m^{-3} ($n_{e0}=1.2\times10^{20}$ m^{-3}). Even in partial CD regimes we are confident to evaluate quite reliably η_{CD}, because in FTU the effect of the residual electric field on the suprathermal electron tail is small, within the experimental errors [13]. The ratio I_{LH}/I_p is evaluated in FTU taking into account the change in the LH phase of the loop voltageand of the bulk conductivity but neglecting the effect of the residual electric field on the fast electron tail. In the quasi steady states considered here, the conductivity is simply proportional to $\langle T_e^{3/2} \rangle$ (<..> stands for volume average) and inversely proportional to Z_{eff} since the internal inductive effects are negligible and the electric field is almost radially uniform, therefore:

$$\frac{I_{LH}}{I_p} = 1 - \frac{V_{l,LH}}{V_{l,OH}} \cdot \frac{\left\langle T_{e,LH}^{3/2} \right\rangle}{\left\langle T_{e,OH}^{3/2} \right\rangle} \cdot \frac{Z_{eff,OH}}{Z_{eff,LH}} \qquad (1)$$

The efficiency for a clean plasma (Z_{eff}=1) η_{CD} is then obtained taking into account the effect of the impurities on the CD, efficiency predicted by quasilinear-theory which yields $\eta_{CD}^{theory} \propto (Z_{eff}+5)^{-1}$

Only the cases with a first penetration inside r/a=2/3 have been selected. Indeed, as soon as this condition is violated, either by lowering B_T or $N_{||0}$, the peak value of the LH $N_{||}$ spectrum ($N_{||}$ is the index of refraction parallel to B_T), or by increasing $\bar{n}_e$, the experimental CD efficiency drops substantially. Data are presented in Fig. 8, where the η_{CD} values are plotted versus <T_e>. The favourable scaling in FTU of the CD efficiency with the electronic temperature is evident, and it has been confirmed directly during the preliminary experiments of combined LHCD + electron cyclotron heating [14].

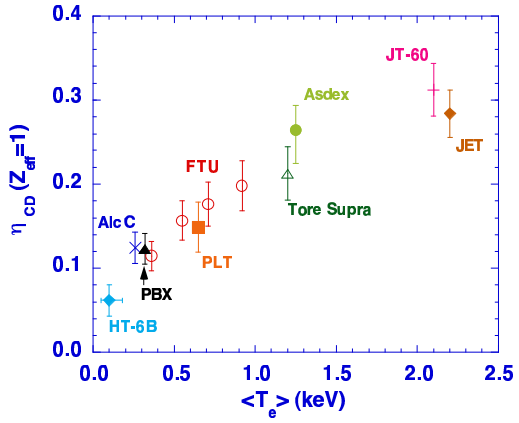

FIG. 9 - Comparison of the highest values of the CD efficiency on various tokamaks as a function of the volume averaged electron temperature $\langle T_e \rangle$: PBX, PLT, HT-6B, Asdex, Tore-Supra, JET, JT-60, Alcator C, FTU. For Alcator C the result for $\bar{n}_e = 1 \cdot 10^{20}\,m^{-3}$ is considered. The vertical bars indicate the range of results obtained for the given $\langle T_e \rangle$.

The positive trend of η_{CD} with $\langle T_e \rangle$ applies to all tokamaks [13], as shown in Fig. 9 where the η_{CD} values, extrapolated to clean plasma conditions (Z_{eff}=1), from the coldest (HT-6B [15]) to the hottest (JET [9]) device are plotted versus $\langle T_e \rangle$. The data are selected in the range $1.7 \le N_{||0} \le 1.9$, if available, otherwise, they are corrected for the different LH phase velocity. The largest $\langle T_e \rangle$ interval available in the literature is examined, and the highest reported efficiencies are considered, except for Alcator C for which η_{CD} is taken at $\bar{n}_e = 1 \times 10^{20}$ m^{-3}. These results are in qualitative agreement with theoretical expectations [16]. LHCD was also used for current profile control. Sawtooth oscillations were stabilised at low density ($n_e < 0.6 \times 10^{20}$ m^{-3}) for values of the loop voltage drop larger then 60% and at high density (($n_e > 0.8 \times 10^{20}$ m^{-3}) even at lower values [17]. Negative central shear configurations in low temperature plasmas were achieved via off-axis LHCD, showing the capability of controlling the power deposition even in a regime where the power absorption at the first ray pass is negligible [16].

4. ELECTRON CYCLOTRON HEATING AND CURRENT DRIVE

The fundamental ω_{ce} resonance (B=5T) with low field side launch in the ordinary polarisation is utilised for the absorption of the Electron Cyclotron wave (ECW). The ECRH system on FTU tokamak is composed of four sub-units, each one with its own gyrotron (140 GHz, 0.5 MW, 0.5 s), polariser (pair of flat corrugated mirrors), transmission line (circular and corrugated, 88.9 mm i.d.) and launching antenna (focusing mirror). Each antenna is steerable both in the vertical and in the toroidal directions [1], for providing off-axis ECW absorption at fixed toroidal magnetic field and electron cyclotron current drive (ECCD).

4.1 High density ECRH

The cut-off electron density in these conditions (140 GHz, fundamental resonance, O-mode) is $n_{e,cut\text{-}off} = 2.4\ 10^{20}$ m^{-3}. The electron temperature in this high density range is $T_{e,0} \approx 1$ keV in typical FTU ohmic discharges ($I_p \approx 700$ kA), which implies that the e-i energy equipartition time (≈10 ms) is less than the global electron energy confinement time (≈30 ms). ECRH experiments have been performed [18] at high density with a single ECRH unit delivering 350kW to the plasma (Fig. 10).

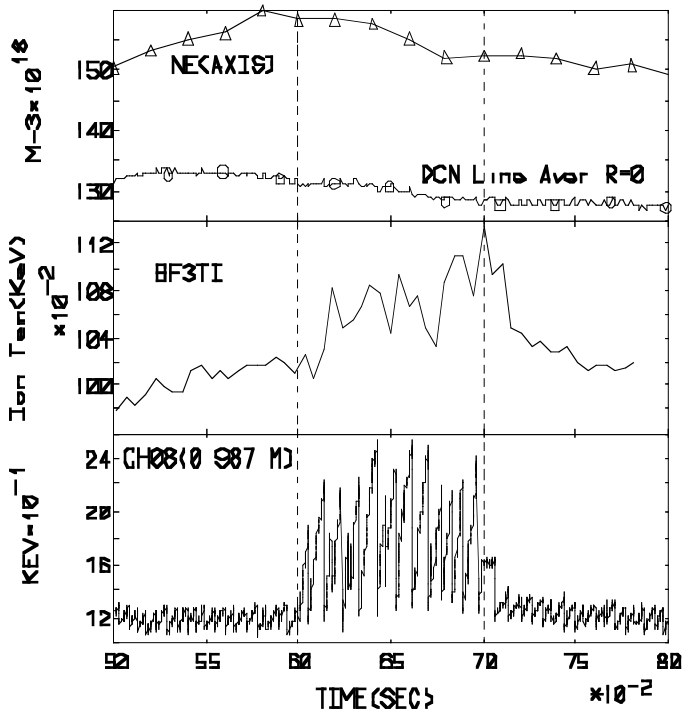

FIG. 10 - Typical electron and ion heating at 350 kW of absorbed ECW power. On-axis ECRH strongly enhances sawteeth. The ion temperature is estimated from D-D neutron emission in a Deuterium discharge. <Te>/Ti ≈ 1.7

The observed rise time of the ion temperature is in agreement with the assumption of a neo-classical e-i collisionality. However, ion energy losses larger by a factor ≈2 than neo-classical have to be accepted to explain the final value of the ion temperature ($\Delta T_i / T_i = 0.1$). It should be noted, however, that the large T_e variations due to sawteeth could induce to an over estimate of the effective average e-i power transfer and, consequently, of the ion diffusivity.

4.2 Localized ECW absorption, electron heating&thermal transport, MHD stabilization

The absorption coefficient for the EC wave propagating into the plasma as an O-mode is significant (≈1.5 cm^{-1}) only within a few cm from the resonance position r_{ris}. Single pass absorption is higher than 95% in most target plasmas provided that $r_{ris}/a \leq 0.5$, where electron temperature and density are high enough to provide significant optical thickness.

The e.m. beam radius, as small as ≈1.8 cm in vacuum, is appreciably increased by refraction only if the peak electron density is close to cut-off (from $n_e/n_{cut\text{-}off} \geq 0.7$). It follows that the size δr of the absorbing volume is small with respect to the plasma radius, being δr/a≈0.2 at worst in most of the experiments.

Localized ECW absorption has been used in FTU to deposit additional heating power in the good confinement region (on-axis ECRH during current ramp-up), to evaluate thermal insulation properties and to control MHD instabilities (sawteeth). Off-axis ECRH, localized at the sawteeth inversion radius, can lead to stabilization due to shear reduction at $r_{q=1}$(Fig. 11). The fast local change in the resistivity forces a flattening of the current density profile inside the absorption radius. Stabilization is eventually lost as the plasma shifts outwards because of the increased pressure, and ECW absorption falls again inside the reconnecting area. Off-axis ECCD with oblique launch can be used to enhance sawteeth stabilization, but this technique is really effective at high power, because of the relatively low current drive efficiency estimated in these conditions: $\eta_{ECCD} = I_{ec}/P_{ec} \approx 10^{-2}$ A/W.

The sawtooth-free phase is suitable for the evaluation of thermal confinement properties by using an interpretative transport code. The value found in the region $0.2 < r/a < 0.4$, where the heat flux is dominated by ECRH and the error due to uncertainties in the ohmic input term is

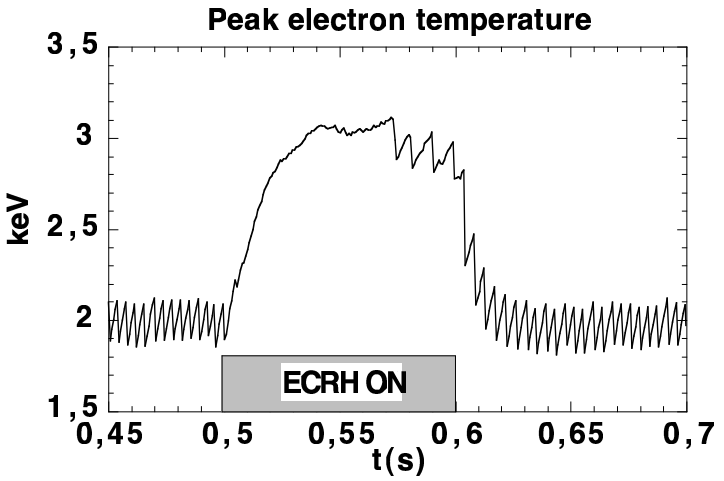

FIG 11 - Sawteeth stabilization with P_{ecrh}=700 kW and rabs ≈ rinv; n_e,line=5 10^{19} m^{-3}; I_p=360 kA; qa≈6; P_{ohmic}=400 kW

negligible, can be as low as $\chi_e \approx 0.4$ m^2/s, very close to the one observed during ECRH on the current ramp-up at about the same plasma current and electron density.

5. ION BERNSTEIN WAVE COUPLING EXPERIMENT

The ion Bernstein wave (IBW) heating scheme utilises the IBW, a hot plasma wave propagating in the range of an ion cyclotron harmonic frequency, for carrying the radiofrequency power in the core of the tokamak plasma and coupling directly on the thermal ions [19]. Moreover, recent theory [20] and experiments [21] have shown that spatially localised IBWs can induce a velocity shear layer useful for core barrier formation via turbulence stabilisation. The IBW experiment on FTU [22, 12] is the first experiment utilising a waveguide antenna similar to the grill antennas of the Lower Hybrid current drive experiments; the IBW scheme needs to launch, in fact, the same slow electron plasma wave. This antenna excites slow electron plasma waves which are expected to mode convert into IBWs near the cold Lower Hybrid resonance layer, which is located in the scrape-off plasma. Furthermore due to the f_0^{-2} dependence of the ponderomotive potential, the higher operating frequency of the IBW-FTU experiment is a special feature which gives this experiment more chances to work free from parasitic phenomena, such as non-linear phenomena, induced in the scrape-off plasma by the electrostatic waves excited by the antenna. so making possible to test the IBW heating scenario via slow wave.

The antenna is fed by a pressurised coaxial transmission line connected to a 433MHz klystron power generator. A vacuum tight alumina window located in the waveguides allows to connect the antenna to the vacuum chamber. The antenna capability to couple the RF power to the plasma has been successfully tested. About 300 kW of RF power, only limited by the present capability of the RF power supply, were coupled to the plasma free from arcing in the antenna. The corresponding RF power density is about 1.3 kW/cm^2; a value in the range of performance expected by extrapolating the best results obtained by the waveguide grill antennas employed in the Lower Hybrid heating and current drive experiments. In order to optimise the antenna coupling, the position of the antenna and the waveguide phasing were changed shot by shot during the experiment. The plasma density at the antenna-plasma interface was monitored by Langmuir probes located at the antenna mouth.

As a result, the RF power reflection coefficient, for a given waveguide phasing, mainly depends on the plasma density measured at the antenna mouth. The best coupling, corresponding to an RF power reflection coefficient of 15%÷20%, is obtained by operating at a plasma density of a few 10^{16} m^{-3} measured a the antenna mouth, and waveguide phasing of about 40°.

A comparison with the results of the model developed for the IBW waveguide antenna coupling [23, 24] is shown in Fig. 12. Both the measured and the expected reflection coefficients increase by increasing the plasma density at the antenna-plasma interface.

Moreover, no direct IBW coupling is found, by operating with plasma densities greater

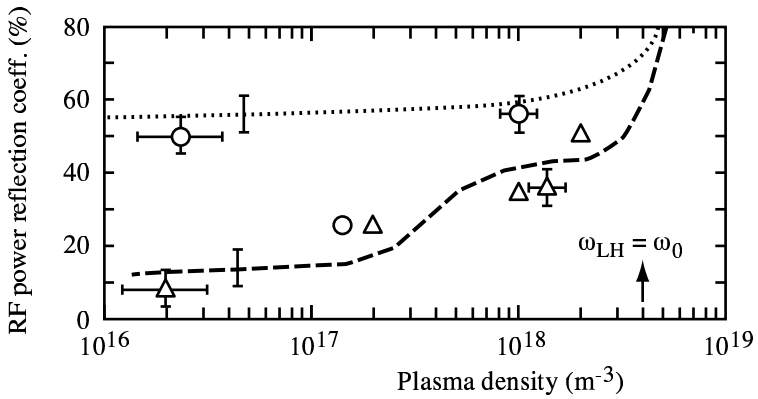

FIG. 12 Comparison of the measured and calculated RF power reflection coefficients of the waveguide antenna, against the plasma density at the antenna-plasma interface. The $\Delta\Phi=0$ radians (dotted line), and $\Delta\Phi=\pi$ radians (dashed line) phasing have been considered in the model. Some measured rf power reflection coefficients, with phasing 0^o-220^o (circles) and a-40^o (triangles), are shown.

than 10^{18} m^{-3} at the grill, as expected by the model. The waveguide phasing which has produced the minimum RF power reflection during the experiment is lower than the value of 180^o, expected by the computation. This difference can be due to a possible effect of wave reflection on the vacuum vessel which can modify the electric field spectrum at the antenna-plasma interface. This effect, not considered in the model, could occur within a range of a few parallel wavelengths from the antenna (50 cm typically).

However the agreement of the measured and the expected RF power antenna reflection trends with the plasma density gives confidence that the antenna can work properly in launching the slow wave necessary for the IBW experiment.

6. IMPURITY TRANSPORT STUDIES

The radial profiles for the diffusive and convective impurity transport coefficients D and V in the plasma core ($0 < r/a < 0.7$) have been obtained by the measurements of the absolute fluxes of a few species of molybdenum ions (Mo^{33+} to Mo^{23+}) under the assumption of steady-state conditions, and compared with the quasilinear expression for the anomalous transport induced by electrostatic turbulence [25]. The *L*-shell emission spectra of Mo^{29+} - Mo^{33+} in the range 4 - 5.5 Å were obtained with a rotating crystal spectrometer. Using a detailed collisional-radiative model developed at LLNL that incorporates *ab initio* atomic calculations [26], we identify a reliable line transition from each ion in each discharge and measure its experimental brightness as a function of impact parameter. From these measurements, it is possible, using the calculated atomic data, to get the radial density profile $N_Z(r)$ for the three ions (Z=32, 31 and 30). Then, the flux Γ_{31+} can be derived from the continuity equation [27], in steady state, from the knowledge of the source terms. Under the assumption that impurities do not alter the background turbulence dynamics (which is correct as long as the impurity concentration is sufficiently low) it is possible to show that the impurity flux can be exactly written as Γ_Z=-D ∇n_Z+Vn_Z, with D and V depending only on the turbulence characteristics and the impurity charge, but being independent of the impurity density. Thus, from the experimental measurements, it is possible to determine the radial profile of D and V. The D nd V profiles have been compared with the theroretical expression obtained from quasilinear theory. The perturbed distribution function for impurities is obtained from the Drift-Kinetic equation using a Krook model for the collision operator. The frequency ω of the fluctuating electric field is taken as a parameter in the calculation. The experimental results are very well reproduced with ω in the range10^5 to 2×10^5 Hz, in agreement with the spectrum of fluctuations expected on FTU. The comparison is shown in Fig. 13.

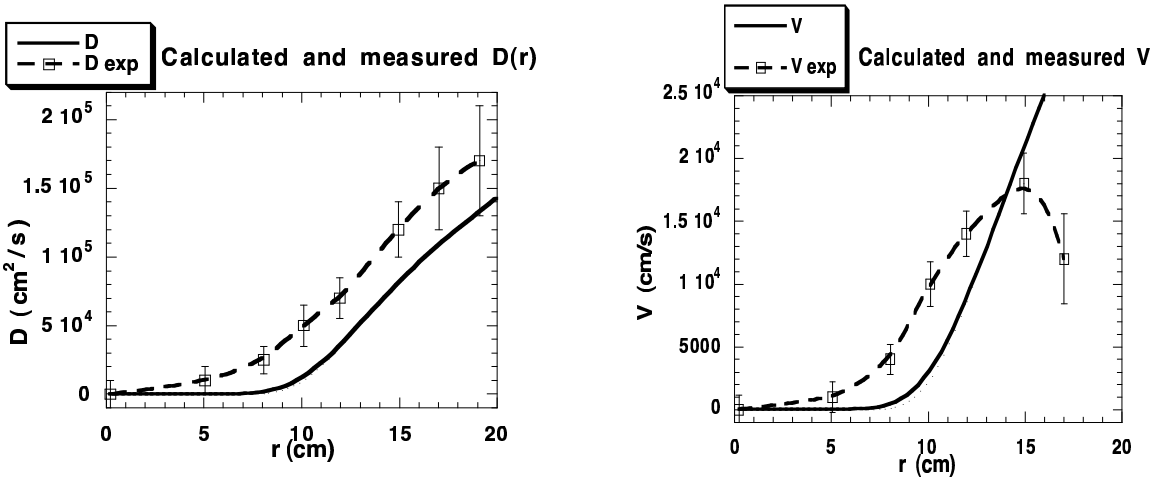

FIG. 13 Diffusion coefficient and convective velocity measured (dotted) and calculated (continuous)

7. FUTURE PLANS

The possibility of modification of FTU in order to study D-shaped plasmas (FTU-D) at high β_p with a large bootstrap fraction is at present under investigation. Elongations up to k=1.6 and high triangularity values can be obtained by a proper programming of the poloidal coils. The plasma will be close to the wall in the outer part. Thus, typical aspect ratio values will be in the range R/a=5.5. The use of the ECRH system constrains the operation to B=2.5T and B=5T. Plasmas with a double X-point well inside the vacuum chamber can be run up to a plasma current around 350kA. In these conditions the bootstrap fraction is expected, on the basis of the ITERH97 [28] scaling, to be in the range 80-90%. Typical plasma parameter are give in Table I.

TABLE I. Plasma parameters of three FTU-D equilibria achievable in the presence of 4MW of heating power. The first two columns refer to separatrix equilibria, namely a 5T equilibrium at the maximum current (col. 1) and a 2.5T equilibrium (col.2) at 250kA. In these two columns only the parameters achievable in the H-mode are shown. On the contrary, column 3 refers to a limiter equilibrium at the maximum current. Both L mode and H mode parameters are shown in this case. The coefficient H-ITER-97 is the improvement factor with respect to L-mode confinement expected on the basis of the H-mode scaling.

	Col. 1	**Col. 2**	**Col. 3**	
	A=5.76 (a= .184m)	A=5.92 (a= .179m)	A=5.4 (a= .216)	
	H-mode	H-mode	L-mode	H-mode
I_P (kA)	350	250	800	
B (T)	5	2.5	5	
k	1.58	1.63	1.39	
q*	4	2.8	2	
H-ITER-97	2.75	2.52	1	2.5
t_E(ms)	48	26	33	82
n_{eLine} ($10^{20}m^{-3}$)	1.4	0.83	1.3	
$<T_e>$ (keV)	2.5	2.4	1.6	3.9
β %	1.16	2.5	0.66	1.6
β_p	3.5	3.7	0.44	1.1
β_N% (mT/MA)	3	4.6	0.9	2.2
f_B	0.96	1	0.13	0.33
t_{skin}(s)	0.77	0.66	0.51	2

The main goals of this experiment will be:

- the investigation of the access to enhanced confinement regimes with additional heating systems which do not fuel the plasma and do not induce a rotation;
- the study of MHD (and neoclassical MHD) stability in the presence of a large bootstrap fraction;
- the achievement and control of advanced scenario configurations on a time scale comparable or larger than the skin time.

Since FTU is mainly equipped with electron heating systems, it will be possible to perform detailed investigations of the electron transport behaviour. This is particularly relevant for burning plasma conditions since the alpha particles heat directly the electron population.

References

[1] CIRANT, S., et al., "Long pulse ECRH experiments at 140 GHz on FTU tokamak", Proc. 10th Joint Workshop on ECE and ECRH, T. Donne' and Toon Verhoeven Editors, 369 (1997).

[2] BRACCO, G., et al., "Energy transport analysis of high temperature and high density FTU plasma discharges", Paper IAEA-F1-CN-69/EXP2/01, these proceedings

[3] VLAD, G., et al., "A general empirically based microinstability transport model", Nucl. Fusion **38** (1998) 557.

[4] BURATTI, P. et al., "MHD activity in FTU plasmas with reversed magnetic shear", Plasma Phys. Contr. Fusion 39, B303 (1997).

[5] BURATTI, P. et al., "MHD studies in FTU plasmas with low and negative magnetic shear", Paper IAEA-F1-CN-69/EXP3/01, these proceedings.

[6] BURATTI, P. et al., "Internal MHD modes in FTU plasmas with high core confinement" 25th EPS Conf. on Controlled Fusion and Plasma Physics, Prague 1998.

[7] TUCCILLO, A.A et al., II Int. Workshop on Strong Microwaves in Plasmas, Nizhny Novgorod, 15-22 August 1993, **V. 1**, p. 47-59

[8] PORKOLAB, M., SCHUSS, J. J., LLOYD, B., et al., Phys. Rev. Lett., **V. 53** , p. 450, (1984)

[9] EKEDHAL, A., BARANOV, Y., DOBBING, J., et al. Proc 23rd EPS Conf. on Plasma Phys. and Controll. Fusion, Kiev, Ukraine, 24 - 28 June 1996, **V.20C**, part II, p. 969

[10] WATARI, T., Plasma Phys. Controll. Fus, **V. 35**, p. A181, (1993)

[11] KNOWLTON S.,. Porkolab, M, Takase, Y. ,et al. Phys. Rev Lett., **V. 57** , p. 587, (1986)

[12] PERICOLI RIDOLFINI V., et al. “High Density Lower Hybrid Current Drive and Ion Bernstein wave heating experiments on FTU” IAEA-F1-CN69/CDP/4 these proceedings

[13] PERICOLI RIDOLFINI, V., et al. Phys. Rev. Lett. to be published

[14] PERICOLI RIDOLFINI, V., CIRANT, S., et al., Proc 24th EPS Conf. on Controll. Fusion and Plasma Phys, Berchtesgaden, Germany, 9 - 13 June 1997, **V21A**, Part III, p. 1157

[15] CAO, Y., et al., Proc. 13th Conf. on Plasma Phys and Controll. Nucl. Fusion Research, Washington DC, USA, 1-6 Oct. 1990, **V. I**, p. 411

[16] BARBATO, E., Plasma Phys. Control. Fusion 40, (1998) A63

[17] TUDISCO O., et al., 2nd Europhysics topical Conference on “Radio Frequency Heating and Current Drive of Fusion Devices, Brussels (Belgium), January 20-23 1998, p. 153

[18] CIRANT S. et al., “Electron Cyclotron Heating at 140 GHz on FTU Tokamak During Current Ramp-Up and Steady-State Conditions” – Paper IAEA-F1-CN69/CD1/3, these proceedings

[19] ONO, M., Phys. Fluids B **2** (1993) 241.

[20] CRADDOCK, G., et al., Phys. Rev. Lett. **67** (1991) 1535.

[21] LEBLANC, B., et al., Phys. Plasmas **2** (1995) 741.

[22] CESARIO, R. et al., and references therein, in 2nd Europhysics Topical Conference on Radio Frequency Heating and Current Drive of Fusion Devices, Brussels (Belgium) 1998, edited by J. Jaquinot, G. Van Oost, R.R. eynants, European Physical Society, brussels (Belgium) 1998, Vol. 22A, p. 65.

[23] CESARIO, R., DE MARCO, F., SAUTER, O., Nuclear Fusion, **38** No. 1 (1998) 31.

[24] CESARIO, R., et al., Nuclear Fusion, 34 **11** (1994) 1527; CARDINALI, A., et al., in Proceedings of the 21st EPS Conference on Controlled Fusion and Plasma Physics, Montpellier, 1994 (European Physical Society, Petit-Lancy, 1994) p. 968;

RUSSEL, D. A., et al., Phys. Plasmas, Vol. 5 No. 3, (1998) 743
[25] PACELLA D. et al. “Impurity Transport Studies on the FTU Tokamak IAEA-CN-69/EXP1/01 these proceedings
[26] FOURNIER, K., PACELLA, D., et al 1996 Phys. Rev. A **54** 3870
[27] PACELLA, D., et al 1997 Plasma Phys. Control. Fusion **39** 1501